A Triad of Variable-Valent Rhenium Aldimine and Amide Systems Interrelated by Successive Oxygen Atom Transfer

Bimal Kumar Dirghangi, Mahua Menon, Amitava Pramanik, and Animesh Chakravorty*

Department of Inorganic Chemistry, Indian Association for the Cultivation of Science, Calcutta 700 032, India

Received September 11, 1996[⊗]

The title systems are $Re^{V}OCl_3$(RA), **1**, $Re^{III}(OPPh_3)Cl_3$(RA), **2**, and $Re^{IV}(OPPh_3)Cl_3$(RB), **3**, where RA is a 2-pyridinecarboxaldimine, *p*-$RC_6H_4N{=}CHC_5H_4N$, and RB^- is the corresponding 2-picolinamide, *p*-$RC_6H_4NC(=O)C_5H_4N^-$ (R = H, Me, OMe, Cl). Controlled reaction of $ReOCl_3(PPh_3)_2$ with RA affords **1**, which is converted to **2** upon reaction with PPh_3. The oxidation of **2** in aqueous media by Ce^{4+} or H_2O_2 furnishes **3**. The X-ray structure of **1** (R = Me) has revealed meridional $ReCl_3$ geometry, the oxo atom lying *trans* to the pyridine nitrogen of chelated MeA. The metal atom is displaced by 0.35 Å toward the oxo atom from the $ReCl_3N$(aldimine) plane. The couples $\mathbf{2}^+/\mathbf{2}$ ($E_{1/2} \sim 0.3$ V *vs* SCE), $\mathbf{3}^+/\mathbf{3}$ ($E_{1/2} \sim 1.3$ V), and $\mathbf{3}/\mathbf{3}^-$ ($E_{1/2} \sim -0.5$ V) are observable electrochemically. The conversion **1** → **2** follows a second-order rate law with a large and negative entropy of activation (∼−40 eu). The reaction is proposed to proceed via nucleophilic attack by the phosphine on Re=O; the observed effects of R and phosphine variation on the rate are consistent with this. In the conversion of **2** to **3**, the active species is $\mathbf{2}^+$, the stoichiometry of the reaction being $3\mathbf{2}^+ + H_2O \rightarrow 2\mathbf{2} + \mathbf{3} + 3H^+$. The amide oxygen in **3** originates from the water molecule. The reaction follows a second-order law, and the entropy of activation is large and negative, ∼−30 eu. The rate-determining addition of water to the aldimine function is believed to afford an α-hydroxy amine intermediate which undergoes induced electron transfer and associated changes, affording **3**. Crystal data for $ReOCl_3$(MeA) are as follows: empirical formula $C_{13}H_{12}Cl_3N_2ORe$; crystal system triclinic; space group $P\bar{1}$; $a = 7.136(4)$ Å, $b = 8.329(5)$ Å, $c = 14.104(9)$ Å, $\alpha = 73.88(5)°$, $\beta = 76.35(5)°$, $\gamma = 85.64(5)°$; $V = 782.5(8)$ Å^3; $Z = 2$.

Introduction

Selective redox transformation of substrates via transfer of oxygen atoms promoted by transition metal variable valence is an abiding theme of chemical research. This work forms part of a program on the synthesis and characterization of new families of variable-valence rhenium compounds that are potential sites of facile oxygen atom transfer reactions. The prevalence of the $Re^{V}O$ motif[1] in rhenium chemistry and its documented ability to participate in oxygen atom transfer[2−6] provided the initial basis for making progress. Herein we report a family of $Re^{V}O$ complexes incorporating chelated 2-pyridinecarboxaldimines. These are remarkable in undergoing oxygen atom transfer in two successive stages at two different sites and in opposite senses. In the first stage, an oxygen atom is transferred *outward* from the $Re^{V}O$ function to an oxophilic substrate like PPh_3, the phosphine oxide thus formed remaining strongly held by the reduced metal site, eq 1. In the second

$$Re^{V}(=O)-\underset{|}{N}=\underset{|}{C}H \xrightarrow{PPh_3} Re^{III}(-OPPh_3)-\underset{|}{N}=\underset{|}{C}H \qquad (1)$$

$$Re^{IV}(-OPPh_3)-\underset{|}{N}=\underset{|}{C}H \xrightarrow{H_2O} Re^{IV}(-OPPh_3)-\underset{|}{N}-\underset{|}{C}=O \qquad (2)$$

stage, the phosphine oxide complex, after oxidation to the Re^{IV} state, undergoes *inward* oxygen atom transfer to the aldimine function from a water molecule. The Re^{IV}(aldimine) group is converted to the Re^{IV}(amide) group in this process, eq 2.[7] The three families of types Re^{V}−aldimine, Re^{III}−aldimine, and Re^{IV}−amide represented by eqs 1 and 2 have been isolated and characterized. The rates and pathways of the two reactions are scrutinized.

[⊗] Abstract published in *Advance ACS Abstracts*, February 1, 1997.

(1) (a) Tsang, B. W.; Reibenspies, J.; Martell, A. E. *Inorg. Chem.* **1993**, *32*, 988. (b) Luo, H.; Rettig, S. J.; Orvig, C. *Inorg. Chem.* **1993**, *32*, 4491. (c) Wang, Y.-P.; Che, C.-M.; Wong, K.-Y.; Peng, S.-M. *Inorg. Chem.* **1993**, *32*, 5827. (d) Shultze, L. M.; Todaro, L. J.; Baldwin, R. M.; Byrne, E. F.; McBride, B. J. *Inorg. Chem.* **1994**, *33*, 5579. (e) Chi, Y.-D.; Wilson, S. R.; Katzenellenbogen, J. A. *Inorg. Chem.* **1995**, *34*, 1624. (f) Tisato, F.; Bandoli, G.; Refso, F.; Bolzati, C. *Inorg. Chem.* **1995**, *34*, 1779. (g) Spies, H.; Fietz, T.; Pietzsch, H. J.; Johannsen, B.; Leibnitz, P.; Reck, G.; Scheller, D.; Klostermann, K. *J. Chem. Soc., Dalton Trans.* **1995**, 2277. (h) Ahmet, M. T.; Lu, C.; Dilworth, J. R.; Miller, J. R.; Zheng, Y.; Hibbs, D. E.; Hursthouse, M. B.; Malik, K. M. A. *J. Chem. Soc., Dalton Trans.* **1995**, 3143. (i) Hansen, L.; Lipowska, M.; Taylor, A.; Marzilli, L. G. *Inorg. Chem.* **1995**, *34*, 3579.

(2) (a) Rouschias, G.; Wilkinson, G. *J. Chem. Soc. A* **1967**, 993. (b) Rowbottom, J. F.; Wilkinson, G. *J. Chem. Soc., Dalton Trans.* **1972**, 826.

(3) (a) Mayer, J. M.; Tulip, T. H. *J. Am. Chem. Soc.* **1984**, *106*, 3878. (b) Bryan, J. C.; Stenkamp, R. E.; Tulip, T. H.; Mayer, J. M. *Inorg. Chem.* **1987**, *26*, 2283.

(4) Fontaine, X. L. R.; Fowles, E. H.; Layzell, T. P.; Shaw, B. L.; Thornton-Pett, M. *J. Chem. Soc., Dalton Trans.* **1991**, 1519.

(5) Holm, R. H. *Chem. Rev.* **1987**, *87*, 1401 and references therein.

(6) Oxygen atom transfer involving rhenium(VII) oxo species has received significant attention: (a) Abu-Omar, M. M.; Espenson, J. H. *J. Am. Chem. Soc.* **1995**, *117*, 272. (b) Herrmann, W. A.; Kühn, F. E.; Rauch, F. E.; Carreia, J. D. G.; Artus, G. *Inorg. Chem.* **1995**, *34*, 2914. (c) DuMez, D. D.; Mayer, J. M. *Inorg. Chem.* **1995**, *34*, 6396. (d) Zhu, Z.; Al-Ajlouni, A. M.; Espenson, J. H. *Inorg. Chem.* **1996**, *35*, 1408.

(7) Preliminary communication: (a) Menon, M.; Pramanik, A.; Bag, N.; Chakravorty, A. *Inorg. Chem.* **1994**, *33*, 403. (b) Menon, M.; Choudhury, S.; Pramanik, A.; Deb, A. K.; Chandra, S. K.; Bag, N.; Goswami, S.; Chakravorty, A. *J. Chem. Soc., Chem. Commun.* **1994**, 57.

S0020-1669(96)01109-3 CCC: $14.00

Table 1. Electronic Spectral[a] and IR[b] Data at 298 K

compd	UV−vis data: λ_{max}, nm (ϵ, M^{-1} cm^{-1})	IR data: ν, cm^{-1}
1(H)	735 (163), 495 (2928)	315, 335; 1010; 1600
1(Me)	730 (222), 490 (2450)	335, 350; 1000; 1610
1(Cl)	720 (105), 490 (2436)	325; 1010; 1600
1(OMe)	730 (226), 490 (3763)	340, 350; 1000; 1610
2(H)	1950 (392), 1500 (225), 680 (1702), 525 (3495), 475[c] (2211), 425[c] (1847)	320; 1120; 1595
2(Me)	1950 (390), 1500 (237), 675 (2200), 525 (4138), 450[c] (2725), 425[c] (2523)	310; 1120; 1600
2(Cl)	1950 (443), 1500 (274), 680 (1916), 525 (3946), 455[c] (2521), 425[c] (2329)	325; 1120; 1600
2(OMe)	1900 (430), 1500 (248), 680 (2418), 525 (4469), 450[c] (3257), 420[c] (3078)	320; 1120; 1600
3(H)	720 (87), 530[c] (534), 400 (2169)	320; 1120; 1600,1640
3(Me)	725 (85), 525[c] (540), 400 (2264)	320; 1120;1600, 1640
3(Cl)	700 (43), 525[c] (730), 400[c] (1597)	320; 1120;1600, 1640
3(OMe)	725 (94), 525[c] (512), 400[c] (2732)	320; 1120;1600, 1635
2$(H)^{+}$ [d]	750 (125), 475 (1680)	
2$(Me)^{+}$ [d]	740 (117), 470 (1550)	

[a] The solvent is dichloromethane except in the case of **2**$(R)^{+}$. [b] In KBr disk; ν_{Re-Cl} 300−350 cm^{-1}, $\nu_{Re=O}$ 1000−1010 cm^{-1}, ν_{PO} 1120 cm^{-1}, $\nu_{C=N}$ 1600−1610 cm^{-1}, $\nu_{C=O}$ 1600−1640 cm^{-1}. [c] Shoulder. [d] Electrogenerated in acetonitrile.

Scheme 1

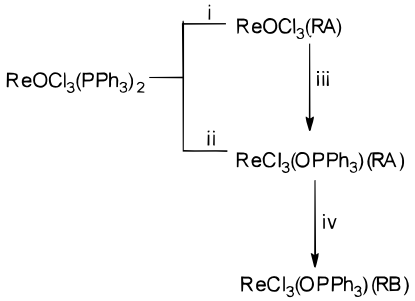

Conditions:
(i) RA, PhMe, warm, 40°C, N_2, 2 min
(ii) RA, PhMe, warm, stir, N_2, 50°C, 10 min
(iii) PPh_3, CH_2Cl_2, stir, 1h ;
(iv) MeCN, $[NH_4]_4[Ce(SO_4)_4].2H_2O$ - H_2O, stir, 2h, or MeCN, 30% H_2O_2, stir, 1h.

Results and Discussion

Synthesis and Characterization. The compound types and their gross geometries as revealed by X-ray work (*vide infra*) are depicted in **1**−**3**. The 2-pyridinecarboxaldimine ligand (in

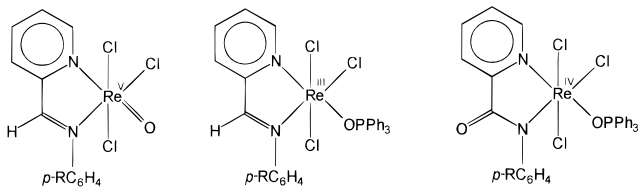

1 and **2**) will be abbreviated as RA (R = H, Me, OMe, Cl), and the monoanionic picolinamide ligand (in **3**), as RB^{-}. A specific compound within the families **1**−**3** will be identified by placing R in parentheses: **1**(H), **2**(OMe), **3**(Cl), etc.

The synthetic methods used are outlined in Scheme 1. Controlled reaction of $ReOCl_3(PPh_3)_2$ with RA in warm toluene affords **1** as a brown solid (orange in solution). If **1** is left in the reaction solution, it is spontaneously converted to **2**, which is isolated as a dark colored solid (pink in solution). Oxidation of **2** in aqueous media furnishes **3** as a brown solid (brown-yellow in solution).

The complexes prepared in this work and their selected spectral features are listed in Table 1. The bands due to electronic transitions in the visible/near-IR region are characteristically different for each compound type and are of diagnostic value as in rate studies (*vide infra*). In IR, the Re−Cl stretches occur in the region 300−350 cm^{-1} while ν_{ReO} and ν_{OP} appear near 1000 and 1100 cm^{-1}, respectively. The aldimine C═N stretch is observed at ∼1600 cm^{-1}, and the amide function displays a pair of strong features near 1600 and 1640 cm^{-1}. Representative magnetic moments and probable gross electronic configurations are as follows: **1**(Me), diamagnetic (d_{xy}^2); **2**(Me),2.84 μ_B ($d_{xy}^2 d_{xz}^1 d_{yz}^1$); **3**(Me), 3.65 μ_B ($d_{xy}^1 d_{xz}^1 d_{yz}^1$).

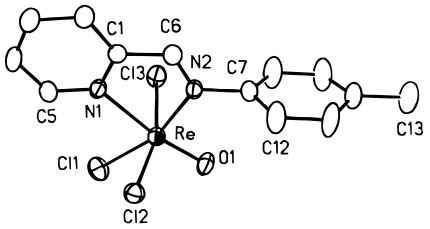

Figure 1. ORTEP plot and atom-labeling scheme for *mer*-$ReOCl_3$(MeA), **1**(Me). All non-hydrogen atoms are represented by 30% probability ellipsoids.

Table 2. Selected Bond Distances (Å) and Angles (deg) and Their Estimated Standard Deviations for *mer*-$ReOCl_3$(MeA), **1**(Me)

	Distances		
Re−N(1)	2.295(8)	Re−N(2)	2.072(10)
Re−Cl(1)	2.318(5)	Re−Cl(2)	2.375(3)
Re−Cl(3)	2.335(3)	Re−O(1)	1.668(9)
N(1)−C(1)	1.354(15)	N(2)−C(6)	1.266(12)
C(1)−C(6)	1.435(18)		
	Angles		
N(1)−Re−N(2)	72.4(4)	N(1)−Re−Cl(1)	89.2(3)
N(2)−Re−Cl(1)	161.3(3)	N(1)−Re−Cl(2)	79.9(2)
N(2)−Re−Cl(2)	91.4(2)	Cl(1)−Re−Cl(2)	88.7(1)
N(1)−Re−Cl(3)	83.6(2)	N(2)−Re−Cl(3)	87.2(3)
Cl(1)−Re−Cl(3)	87.2(1)	Cl(2)−Re−Cl(3)	163.0(1)
N(1)−Re−O(1)	164.2(5)	Cl(1)−Re−O(1)	106.1(4)
Cl(2)−Re−O(1)	96.6(3)	Cl(3)−Re−O(1)	100.4(3)

Structure. The X-ray structure of $ReOCl_3$(MeA), **1**(Me), has been determined. A view along with the atom-numbering scheme is shown in Figure 1, and selected bond parameters are listed in Table 2. In the distorted octahedral coordination sphere, the $ReCl_3$ fragment has meridional geometry. The Cl(1), Cl(2), Cl(3), and N(2) atoms make a virtually perfect plane (mean deviation 0.003 Å) from which the metal atom is displaced by 0.35 Å toward the oxo atom. The chelate ring is excellently planar, and the pyridine moiety is coplanar with it. The tolyl fragment makes a dihedral angle of 98.6° with this plane. The

Table 3. Cyclic Voltammetric Formal Potentials in Acetonitrile (0.1 M Et_4NClO_4) at a Platinum Electrode at 298 K[a–e]

compd	$E_{1/2}$, V (ΔE_p, mV)	compd	$E_{1/2}$, V (ΔE_p, mV)
1(H)	1.76[f]	**2**(Cl)	0.35 (80)
1(Me)	1.72[f]	**2**(OMe)	0.28 (80)
1(Cl)	1.78[f]	**3**(H)	−0.44 (80) 1.30 (80)
1(OMe)	1.68[f]	**3**(Me)	−0.46 (80) 1.26 (80)
2(H)	0.32 (80)	**3**(Cl)	−0.41 (80) 1.33 (80)
2(Me)	0.30(80)	**3**(OMe)	−0.48 (80) 1.20 (80)

[a] The concerned couples are $\mathbf{1}^+/\mathbf{1}$ (Re^{VI}/Re^{V}), $\mathbf{2}^+/\mathbf{2}$ (Re^{IV}/Re^{III}), $\mathbf{3}/\mathbf{3}^-$ (Re^{IV}/Re^{III}), and $\mathbf{3}^+/\mathbf{3}$ (Re^{V}/Re^{IV}). [b] Scan rate 50 mV s^{-1}. [c] $E_{1/2} = {}^1/_2(E_{pa} + E_{pc})$ where E_{pa} and E_{pc} are the anodic and cathodic peak potentials, respectively. [d] $\Delta E_p = E_{pc} - E_{pa}$. [e] Reference electrode, SCE. [f] E_{pa}.

Re═O length, 1.668(9) Å, is normal.[8] The Re−N(1) bond, subject to the *trans* influence of the oxo atom, is much longer than the Re−N(2) length: 2.295(8) and 2.072(10) Å, respectively. For comparison, we note that in $ReO(OEt)Cl_2(py)_2$ (OEt lies *trans* to O) the average Re−N length is 2.138(7) Å.[9]

The structure of $Re(OPPh_3)Cl_3(MeA)$, **2**(Me), is known.[7a] It has the same gross meridional geometry as **1**(Me). In what follows, the same atom-numbering scheme is used for **1**(Me) and **2**(Me). The most conspicuous changes in going from **1**(Me) to **2**(Me) are (i) a 0.29 Å descent of the metal atom toward the plane of Cl(1), Cl(2), Cl(3), and N(2) (in **2**(Me) the atoms lie only 0.06 Å above the plane) (ii) a 0.41 Å increase of the Re−O length (2.080(4) Å in **2**(Me)), and (iii) a 0.27 Å decrease in the Re−N(1) length (2.030(5) Å in **2**(Me)). These effects are consistent with the change in Re−O bond order (ideally two in **1**(Me) and one in **2**(Me)) and the associated change in *trans* influence. A computer-generated superposition diagram of the coordination spheres in **1**(Me) and **2**(Me) is depicted in **4**. The

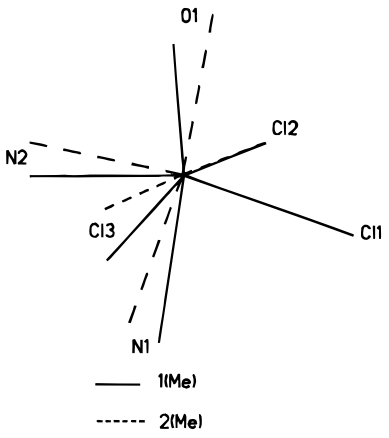

4

Re−N(2) length in **1**(Me) is 0.04 Å longer than that in **2**(Me) even though the metal oxidation state is higher in the former complex. On the other hand, the aldimine N(2)−C(6) length in **1**(Me) is shorter (by 0.06 Å) than that in **2**(Me). Rhenium(III) is a potent π-base,[10] and the observed bond length trends are consistent with the presence of $d\pi(Re^{III}) \rightarrow p\pi^*$(azomethine) back-bonding in **2**(Me). Such back-bonding is not expected to be significant in the pentavalent (d^2) complex **1**(Me). The structure of the amide complex **3**(Me) is also known. The gross geometrical features are similar to those of **2**(Me), the superior back-bonding ability of rhenium(III) being again reflected in bond parameters.[7a]

(8) Mayer, J. M. *Inorg. Chem.* **1988**, *27*, 3899.
(9) Lock, C. J. L.; Turner, G. *Can. J. Chem.* **1977**, *55*, 333.
(10) Ghosh, P.; Pramanik, A.; Bag, N.; Chakravorty, A. *J. Chem. Soc., Dalton Trans.* **1992**, 1883.

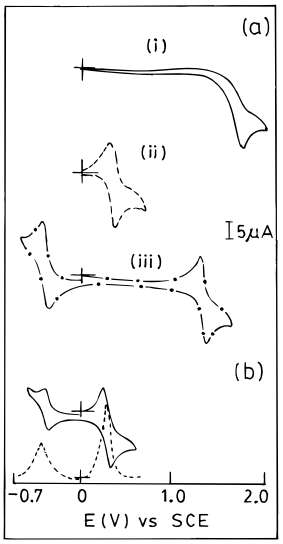

Figure 2. (a) Cyclic voltammograms of a $\sim 10^{-3}$ M solution of (i) $ReOCl_3(MeA)$, (ii) $Re(OPPh_3)Cl_3(MeA)$, and (iii) $Re(OPPh_3)Cl_3(MeB)$ in acetonitrile (0.1 M Et_4NClO_4) at a platinum electrode with a scan rate of 50 mV s^{-1}. (**b**) Cyclic (—) and differential pulse (- - -) voltammograms of the product of the completed reaction of $Re(OPPh_3)Cl_3(MeA)^+$ with water in acetonitrile solution. The two responses (current heights 2:1) correspond to the couples $\mathbf{2}(Me)^+/\mathbf{2}$ (Me) (higher potential) and $\mathbf{3}(Me)/\mathbf{3}(Me)^-$ (lower potential).

Electrochemical Metal Redox. All the three families are electroactive in acetonitrile solution at a platinum electrode. Cyclic voltammetric reduction potential data are collected in Table 3, and representative voltammograms are shown in Figure 2a. The oxo complexes of type **1** display a well-defined anodic peak near 1.7 V *versus* SCE, the peak height corresponding to the transfer of one electron. No corresponding cathodic peak is observable. The anodic peak is tentatively assigned to the oxidation of $Re^{V}O$ to $Re^{VI}O$, the hexavalent complex being unstable on the cyclic voltammetric time scale (hence, no cathodic response on scan reversal).

In complexes of type **2**, the rhenium(IV)−rhenium(III) couple, eq 3, occurs as a quasireversible one-electron response near 0.3

$$\mathbf{2}^+ + e \overset{\sim 0.3\ V}{\rightleftharpoons} \mathbf{2} \qquad (3)$$

V. The potential changes with R, becoming more positive as the electron-withdrawing power increases: OMe < Me < H < Cl (Table 3). The plot of $E_{1/2}$ *versus* Hammett σ is linear with a correlation coefficient of 0.99 ($\rho = 0.14$).

The yellow rhenium(IV) complex cation $Re(OPPh_3)Cl_3(RA)^+$, $\mathbf{2}^+$ (eq 3), has been quantitatively generated in dry acetonitrile solutions in the cases of R = H and Me, by constant-potential coulometry of **2** at 0.5 V. The cyclic voltammogram (initial scan cathodic), of $\mathbf{2}^+$ is superposable on that of the corresponding type **2** complex (initial scan anodic), implying that the transformation of eq 3 is stereoretentive. The electronic spectral data for electrogenerated $\mathbf{2}(H)^+$ and $\mathbf{2}(Me)^+$ are listed in Table 1. The $\mathbf{2}^+$ complexes are crucial (*vide infra*) for the aldimine → amide conversion of eq 2. It has not been possible to isolate $\mathbf{2}^+$ in the pure state as a salt.

The amide complexes of type **3** exhibit successive quasireversible rhenium(IV)−rhenium(III) and rhenium(V)−rhenium(IV) couples near −0.5 V and 1.3 V respectively, eq 4. For a given R, the rhenium(IV)−rhenium(III) reduction

$$\mathbf{3} + e \overset{\sim -0.5\ V}{\rightleftharpoons} \mathbf{3}^- \qquad (4a)$$

$$\mathbf{3}^+ + e \overset{\sim 1.3\ V}{\rightleftharpoons} \mathbf{3} \qquad (4b)$$

potential decreases by a remarkable ~0.8 V in going from **2** (eq 3) to **3** (eq 4a), reflecting the strong stabilization of the tetravalent state by the amide function. Because of the large depression of the rhenium(IV)−rhenium(III) potential, the $Re^{III}(OPPh_3)Cl_3(RB)^-$ species, $\mathbf{3}^-$, electrogenerated in solution is spontaneously oxidized in air, affording **3**. In contrast, **2** is stable in air.

Stoichiometry of Reactions. The oxo transfer reaction **1** → **2** has a simple 1:1 stoichiometry between the reactants **1** and PPh_3, eq 5. In the conversion of **2** → **3** by oxidants in

$$\mathbf{1} + PPh_3 \xrightarrow{k_5} \mathbf{2} \qquad (5)$$

$$3\mathbf{2}^+ + H_2O \xrightarrow{k_6} 2\mathbf{2} + \mathbf{3} + 3H^+ \qquad (6)$$

aqueous media (Scheme 1), the active complex is $\mathbf{2}^+$ formed from **2** via one-electron oxidation. Electrogenerated solutions of $\mathbf{2}^+$ are well-preserved in dry acetonitrile. However upon addition of water to the solution, spontaneous transformation to the amide complex occurs according to the reaction of eq 6. The 2:1 ratio of **2** and **3** in the product at the completion of the reaction is neatly revealed in the voltammogram of Figure 2b. The measurement was made by dissolving in acetonitrile the residue left after removal of solvent and water at the end of the reaction. Spectrophotometry of the product solution is also consistent with the stoichiometry of eq 6.

In the presence of an external oxidant, as in the synthesis of **3** in Scheme 1, the aldimine → amide conversion becomes quantitative, eq 7, because it is no longer necessary for $\mathbf{2}^+$ to act as an oxidant (eq 6).

$$\mathbf{2} + Ce^{4+} \rightarrow \mathbf{2}^+ + Ce^{3+} \qquad (7a)$$

$$\mathbf{2}^+ + H_2O + 2Ce^{4+} \rightarrow \mathbf{3} + 2Ce^{3+} + 3H^+ \qquad (7b)$$

Rate and Activation Parameters. The rates of the reactions of eq 5 and eq 6 have been studied spectrophotometrically in dichloromethane and acetonitrile solutions respectively, using the absorbance at 680 nm (growth of **2**). The spectral time evolution for the **1**(Me) → **2**(Me) conversion at 299 K has been deposited in the Supporting Information as Figure S1a. For this reaction, variable-temperature rate studies have been performed over the range 287−299 K. In addition, the **1**(H) → **2**(H) and **1**(Cl) → **2**(Cl) reactions have been examined at 299 K. The reaction $\mathbf{2}(H)^+ \rightarrow \mathbf{3}(H)$ has been monitored at variable temperatures (280−299 K) and the reaction $\mathbf{2}(Me)^+ \rightarrow \mathbf{3}(Me)$ at 299 K.

Under pseudo-first-order conditions (excess PPh_3 in eq 5 and excess H_2O in eq 6), the rates of reactions 5 and 6 are respectively proportional to the concentrations of **1** and $\mathbf{2}^+$. The observed rate constants k_{5obs} and k_{6obs} are in turn proportional to the concentrations of PPh_3 and H_2O, respectively. The rates are thus second-order in both cases, eqs 8 and 9. Rate constants

$$\mathbf{1} \rightarrow \mathbf{2}\text{: rate} = k_{5obs}[\mathbf{1}] = k_5[\mathbf{1}][PPh_3] \qquad (8)$$

$$\mathbf{2}^+ \rightarrow \mathbf{3}\text{: rate} = k_{6obs}[\mathbf{2}^+] = k_6[\mathbf{2}^+][H_2O] \qquad (9)$$

and activation parameters are collected in Tables 4 and 5 and Eyring plots are shown in the Supporting Information, Figure S1b. Both the reactions are characterized by a large negative entropy of activation in the range −30 to −40 eu, suggesting strong association between **1** and PPh_3 and between $\mathbf{2}^+$ and H_2O in the rate-determining steps of the conversions **1** → **2** and $\mathbf{2}^+$ → **3**, respectively.

Table 4. Rate Constants and Activation Parameters[a] for the Reaction **1**(R) → **2**(R) in Dichloromethane[b,c]

R	*T*, K	$[PPh_3]$, M	10^4k_{obs}, s^{-1}	10^3k, $M^{-1}\ s^{-1}$
Me	287	0.014	0.57	4.11 (0.09)
		0.017	0.70	
		0.022	0.90	
	291	0.014	0.78	5.62 (0.02)
		0.017	0.95	
		0.022	1.23	
	295	0.014	0.98	6.98 (0.06)
		0.017	1.20	
		0.022	1.54	
	299	0.014	1.10	7.96 (0.03)
		0.017	1.36	
		0.022	1.74	
H	299	0.014	1.70	12.26 (0.05)
		0.017	2.08	
		0.022	2.69	
Cl	299	0.014	3.35	24.02 (0.04)
		0.017	4.08	
		0.022	5.30	

[a] For R = Me: $\Delta H^{\ddagger}$, 8.91 (0.25) kcal mol^{-1}; $\Delta S^{\ddagger}$, −38.69 (0.85) eu. [b] Initial concentration of **1** (R) (2.4−2.7) × 10^{-4} M. [c] Least-squares deviations are given in parentheses.

Reaction Models. a. The Reaction 1 → 2. In a simplified description the metal−oxo bond (*z* axis) is taken to be constituted of $5d_{xz}$, $5d_{yz}$(Re) and $2p_x$, $2p_y$(O) orbitals. The reaction can be initiated by nucleophilic PPh_3 attack on the π^* ReO orbital, eventually causing a heterolytic cleavage of the π-bond. The result is a two-electron metal reduction with concomitant engagement of the "freed" oxygen orbital (after suitable rehybridization) in forming a σ-bond with PPh_3 as depicted in **5**. In crystalline **2**(Me) the phosphorus atom lies

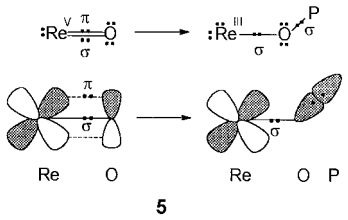

5

1.45 Å from the plane of the octahedral O(1)Cl(1)Cl(2) face such that its nonbonded distances from Cl(1) and Cl(2) are 3.78 and 3.90 Å, respectively.[11] It is conceivable that the direction of the initial approach of PPh_3 is approximately the same as indicated by its above-noted final location in **2**(Me).

The presence of electron-withdrawing groups in **1** is expected to hasten the reaction by facilitating the nucleophilic attack by PPh_3. This does in fact happen, as can be seen in the variation of k_5 with R in the order Cl > H > Me (Table 4). Indeed, the plot of log k_5(299 K) *versus* the Hammett constant of R is excellently linear with a correlation coefficient of 0.99. Increase of phosphine basicity can also be expected to increase the rate of the reaction. We have chosen $PMePh_2$ as the more basic phosphine and studied the reaction[12] of eq 9 at 295 K at

(11) In **3**(Me) the phosphorus atom is similarly located, the corresponding distances being 1.32, 3.98, and 3.98 Å, respectively. The parameters were computed with the help of available atomic coordinates.[7a]

(12) The complex $Re(OPMePh_2)Cl_3(MeA)$ has been isolated and characterized. Anal. Calcd for $C_{26}H_{25}N_2Cl_3OPRe$: C, 44.28; H, 3.55; N, 3.97. Found: C, 44.31; H, 3.58; N, 3.95. UV−vis (CH_2Cl_2): λ = 1900 nm (ϵ = 375), 1500 (300), 675 (1806), 525 (3587), 450 sh (2498) (sh = shoulder), 415 sh (2340). $E_{1/2}$ = 0.32 V(ΔE_p = 80 mV) in CH_3CN.

Table 5. Rate Constants and Activation Parameters[a] for the Reaction $\mathbf{2}^+(R) \rightarrow \mathbf{3}(R)$ in Acetonitrile[b,c]

R	*T*, K	$[H_2O]$, M	10^3k_{obs} s^{-1}	10^3k, M^{-1} s^{-1}
H	280	1.11	0.32	0.25 (0.02)
		1.67	0.48	
		2.22	0.64	
		2.78	0.73	
H	288	1.11	0.53	0.54 (0.04)
		1.67	0.91	
		2.22	1.12	
		2.78	1.47	
H	293	1.11	0.92	0.84 (0.02)
		1.67	1.38	
		2.22	1.81	
		2.78	2.33	
H	296	1.11	1.04	1.02 (0.02)
		1.67	1.58	
		2.22	2.19	
		2.78	2.72	
H	299	1.11	1.29	1.19 (0.01)
		1.67	1.97	
		2.22	2.61	
		2.78	3.29	
Me	299	1.11	0.85	0.69 (0.02)
		1.67	1.26	
		2.22	1.65	
		2.78	2.00	

[a] For R = H: $\Delta H^{\ddagger}$, 13.4 (1.6) kcal mol^{-1}; $\Delta S^{\ddagger}$, −27.3 (0.6) eu. [b] Initial concentration of $\mathbf{2}^+(R)$ 6.6×10^{-4} M. [c] Least-squares deviations are given in parentheses.

phosphine concentrations of 0.0074, 0.0099, and 0.0129 M, affording 10^3k_{10obs} values of 0.33, 0.45, and 0.61 s^{-1}. The

$$\mathbf{1}(Me) + PMePh_2 \xrightarrow{k_{10}} Re(OPMePh_2)Cl_3(MeA) \quad (10)$$

corresponding rate constant k_{10} is 4.70×10^{-2} M^{-1} s^{-1}, which is nearly 7 times larger than the rate constant k_5 of the PPh_3 reaction (Table 4).

In proposing the above model, we have drawn analogy from the biologically relevant oxo-transfer reactions of $Mo^{VI}O_2$ species, eq 11 (L = ligand(s); X = alkyl/aryl).[13−16] In the

$$LMo^{VI}O_2 + PX_3 \xrightarrow{D} LMo^{IV}(=O)D + OPX_3 \quad (11)$$

reaction of eq 11, the phosphine oxide is only weakly bonded to the $Mo^{IV}O$ product, and it undergoes facile displacement by other donors (D) such as water. On the other hand, in the reaction $\mathbf{1} \rightarrow \mathbf{2}$, the phosphine oxide remains strongly bound to the metal, cogently demonstrating that phosphine oxide is indeed formed in the coordinated state. Interestingly, both $Re^{V}O$ and $Mo^{IV}O$ have an nd^2 configuration but the latter is not a good oxo donor toward PX_3 (unfavorable $Mo^{IV}-Mo^{II}$ reduction potential). Indeed, $Mo^{IV}O$ is an oxo acceptor which makes the $Mo^{VI}O_2-Mo^{IV}O$ pair a potent oxo transfer catalyst.

b. The Reaction $\mathbf{2}^+ \rightarrow \mathbf{3}$. In this reaction (eq 6), the amide oxygen atom originates from water. The reaction proceeds unhindered in the absence of dioxygen. The rate-determining step (rds) is the addition of water to the aldimine function. This can be initiated via the nucleophilic attack by the H_2O oxygen on the π^* aldimine orbital. Such an attack is expected to be more facile in $\mathbf{2}^+$ than in **2** because of the lower electron density in the aldimine region in $\mathbf{2}^+$. This lowering occurs because of the higher electron-withdrawing power (higher oxidation state) and lower back-bonding ability (*vide supra*) of rhenium(IV) ($\mathbf{2}^+$) compared to rhenium(III) (**2**). In practice, **2** does not react with water at all, but $\mathbf{2}^+$ does. The rate is higher in the case of $\mathbf{2}(H)^+$ compared to $\mathbf{2}(Me)^+$ (Table 5), consistent with the electron-withdrawing order H > Me. Water addition presumably leads to the α-hydroxy amine intermediate **6**. Stable aquo adducts of Schiff bases have been isolated in certain cases.[17,18]

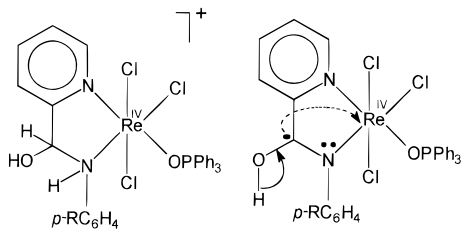

6 **7**

The intermediate **6** has to undergo oxidation rapidly enough to bypass the possible hydrolysis route.[19] This can happen via induced transfer of two electrons[20] eventually leading to **3**. The plausible steps (eq 12) are $\mathbf{6} \rightarrow \mathbf{7}$ (oxidative radical formation

$$\mathbf{2}^+ + H_2O \rightarrow \mathbf{6} \quad (12a)$$

$$\mathbf{2}^+ + \mathbf{6} \rightarrow \mathbf{7} + 2H^+ + \mathbf{2} \quad (12b)$$

$$\mathbf{7} \rightarrow \mathbf{3}^- + H^+ \quad (12c)$$

$$\mathbf{2}^+ + \mathbf{3}^- \rightarrow \mathbf{3} + \mathbf{2} \quad (12d)$$

and proton dissociation), $\mathbf{7} \rightarrow \mathbf{3}^-$ (internal redox and proton dissociation), and $\mathbf{3}^- \rightarrow \mathbf{3}$ (metal oxidation). The oxidant in these steps is $\mathbf{2}^+$. The net result of the sequence of eq 12 is eq 6. In a related system[21] we have good evidence for an intermediate of type **7**.

In this proposal, a crucial requirement is the accessibility of two oxidation states (here Re^{3+} and Re^{4+}) related by facile one-electron transfer which is expressed in the rapid internal redox process. The higher state is such as to be able to affect sufficient electron withdrawal from the aldimine function, ensuring nucleophilic water attack. Aldimine → amide oxidation has earlier been documented in ruthenium[22] and iron[23] chemistry.

Concluding Remarks

The synthesis and structural characterization of a new family of $Re^{V}O$ complexes of type **1** have been achieved. These are remarkable in undergoing successive oxygen atom transfer of two types: *outward* from **1** to a PPh_3 molecule, affording **2**, and *inward* into $\mathbf{2}^+$ from a water molecule, furnishing **3**. Both reactions are associated with a large and negative entropy of activation. The associative pathways are believed to originate from the nucleophilic attack of PPh_3 on Re=O and of water on

(13) Enemark, J. H.; Young, C. G. *Adv. Inorg. Chem.* **1993**, *43*, 1.
(14) Schultz, B. E.; Holm, R. H. *Inorg. Chem.* **1993**, *32*, 4244.
(15) Topich, J.; Lyon, J. T., III. *Inorg. Chem.* **1984**, *23*, 3202.
(16) Pietsch, M. A.; Hall, M. B. *Inorg. Chem.* **1996**, *35*, 1273.
(17) (a) Harris, C. M.; McKenzie, E. D. *Nature*, **1962**, *196*, 670. (b) Busch, D. H.; Bailer, J. C., Jr. *J. Am. Chem. Soc.* **1956**, *78*, 1137. (c) Katovic, V.; Vergez, S. C.; Busch, D. H. *Inorg. Chem.* **1977**, *16*, 1716.
(18) Bandoli, G.; Gerber, T. I. A.; Jacobs, R.; du Preez, J. G. H. *Inorg. Chem.* **1994**, *33*, 178.
(19) Keyser, R. H.; Pollack, R. M. *J. Am. Chem. Soc.* **1977**, *99*, 3379.
(20) Taube, H. *Electron Transfer Reactions of Complex Ions in Solution*; Academic Press: New York, 1973; p 73.
(21) Dirghangi, B. K.; Menon, M.; Pramanik, A.; Chakravorty, A. Unpublished work.
(22) Menon, M.; Pramanik, A.; Chakravorty, A. *Inorg. Chem.* **1995**, *34*, 3310.
(23) (a) Chum, H. L.; Krumholtz, P. *Inorg. Chem.* **1974**, *13*, 519. (b) Chum, H. L.; Helene, M. E. M. *Inorg. Chem.* **1980**, *19*, 876 and references therein.

C═N. Consistent with this, the rates are responsive to variation of the substituent in **1** and $\mathbf{2}^{+}$.

The three systems **1**−**3** represent stabilization of three levels of rhenium oxidation states. In the presence of oxo coordination, the RA ligand is compatible with rhenium(V) as in **1**. Once the oxo group is converted to phosphine oxide, RA stabilizes the +3 state as in **2**. On the other hand, RB^{-} stabilizes rhenium(IV) as in **3**. Between **2** and **3**, the rhenium(IV)−rhenium(III) reduction potential decreases by nearly 1 V. Stabilization of higher oxidation states is a characteristic feature of amide chelation,[24] but there are few known examples in rhenium chemistry outside **3**. Our search for newer rhenium species capable of undergoing oxygen atom transfer reactions is continuing.

Experimental Section

Materials. $ReOCl_3(PPh_3)_2$[25] and 2-pyridinecarboxaldimines[26] were prepared by reported methods. The purification and drying of dichloromethane and acetonitrile for synthesis as well as electrochemical and spectral work were done as before.[27] Toluene was distilled over sodium, before use. All other chemicals and solvents were of reagent grade and were used as received.

Physical Measurements. Electronic spectra were recorded with a Hitachi 330 spectrophotometer fitted with a thermostated cell compartment. Infrared spectra (4000−300 cm^{-1}) were recorded on a Perkin-Elmer 783 spectrometer. Electrochemical measurements (cyclic voltammetry, coulometry, and differential pulse voltammetry) were performed using a PAR Model 370−4 electrochemistry system as described elsewhere.[28] All experiments were performed at a platinum working electrode under a dinitrogen atmosphere, the supporting electrolyte being tetraethylammonium perchlorate (Et_4NClO_4, TEAP). The potentials are referred to a saturated calomel electrode (SCE) and are uncorrected for junction contribution. Magnetic susceptibilities were measured on a PAR 155 vibrating-sample magnetometer. Microanalyses (C, H, N) were performed using a Perkin-Elmer 240C elemental analyzer.

Synthesis of *mer*-$ReOCl_3$(RA), 1. The complexes were prepared by the same general method. Details are given for one representative case. Yields were in the range 25−40%.

***mer*-Trichlorooxo(*N*-*p*-tolyl-2-pyridinecarboxaldimine)rhenium(V), *mer*-$ReOCl_3$(MeA), 1(Me).** The complex $ReOCl_3(PPh_3)_2$ (100 mg, 0.12 mmol) was suspended in 10 mL of dry toluene, and nitrogen gas was passed through the suspension for 15 min. The suspension was then warmed to 40 °C, and a solution of MeA (35 mg, 0.18 mmol) dissolved in 5 mL of toluene was added. The mixture was kept at 40 °C for 2 min (it is necessary to control the time carefully; otherwise transformation to **2**(Me) occurs), and the brown microcrystalline solid that precipitated was collected by filtration, washed thoroughly with diethyl ether, and finally dried in vacuo over P_4O_{10}. Yield: 23 mg, 39% (unavoidable formation of some **2**(Me) is responsible for the low yield). Anal. Calcd for $ReOCl_3$(MeA), $ReC_{13}H_{12}N_2Cl_3O$: C, 30.93; H, 2.40; N, 5.54. Found: C, 30.89; H, 2.49; N, 5.51.

Anal. Calcd for $ReOCl_3$(HA), $ReC_{12}H_{10}N_2Cl_3O$: C, 29.35; H, 2.04; N, 5.71. Found: C, 29.43; H, 2.00; N, 5.78. Calcd for $ReOCl_3$(ClA), $ReC_{12}H_9N_2Cl_4O$: C, 27.43; H, 1.71; N, 5.33. Found: C, 27.36; H, 1.76; N, 5.40. Calcd for $ReOCl_3$(OMeA), $ReC_{13}H_{12}N_2Cl_3O_2$: C, 29.97; H, 2.31; N, 5.38. Found: C, 30.04; H, 2.25; N, 5.30.

Synthesis of *mer*-$Re(OPPh_3)Cl_3$(RA), 2. The complexes could be prepared directly from $ReOCl_3(PPh_3)_2$ or from $ReOCl_3$(RA) in 80−95% yields. Details are given for a representative case. Usually the $ReOCl_3(PPh_3)_2$ route was utilized.

***mer*-Trichloro(triphenylphosphine oxide)(*N*-*p*-tolyl-2-pyridinecarboxaldimine)rhenium(III), *mer*-$Re(OPPh_3)Cl_3$(MeA), 2(Me). a. From $ReOCl_3(PPh_3)_2$.** A 100 mg (0.12 mmol) sample of $ReOCl_3(PPh_3)_2$ was suspended in 30 mL of dry freshly distilled toluene, and a stream of nitrogen gas passed through the suspension for 15 min. The mass was warmed to about 50 °C, and to it was added MeA (35 mg, 0.18 mmol) dissolved in 5 mL of toluene. The mixture was then stirred at 50 °C for 10 min. The resulting solution was filtered off, and the pink filtrate was evaporated to dryness under reduced pressure. The solid mass thus obtained was dissolved in 5 mL of dichloromethane and the solution subjected to chromatography on a silica gel column (20 × 1 cm; 60−120 mesh, BDH). Upon elution with benzene, a small yellow band separated out, which was rejected. The pink band that followed was eluted with a benzene−acetonitrile (20:1) mixture. The required complex was obtained from the eluate as shining dark microcrystals, by slow evaporation. Yield: 78 mg, 85%. Anal. Calcd for $Re(OPPh_3)Cl_3$(MeA), $ReC_{31}H_{27}N_2Cl_3OP$: C, 48.53; H, 3.52; N, 3.65. Found: C, 48.48; H, 3.56; N, 3.70.

b. From $ReOCl_3$(RA). To a solution of $ReOCl_3$(MeA) (50 mg, 0.10 mmol) dissolved in dichloromethane was added an excess of PPh_3 (250 mg, 0.95 mmol). The mixture was stirred for 1 h. Evaporation of the solvent under reduced pressure gave a dark product. This, upon repeated washing with hexane, afforded $Re(OPPh_3)Cl_3$(MeA) in nearly quantitative yield (∼95%).

Anal. Calcd for $Re(OPPh_3)Cl_3$(HA), $ReC_{30}H_{25}N_2Cl_3OP$: C, 47.84; H, 3.32; N, 3.72. Found: C, 47.81; H, 3.29; N, 3.68. Calcd for $Re(OPPh_3)Cl_3$(ClA), $ReC_{30}H_{24}N_2Cl_4OP$: C, 45.74; H, 3.05; N, 3.56. Found: C, 45.82; H, 2.98; N, 3.50. Calcd for $Re(OPPh_3)Cl_3$(OMeA), $ReC_{31}H_{27}N_2Cl_3O_2P$: C, 47.54; H, 3.45; N, 3.58. Found: C, 47.60; H, 3.40; N, 3.52.

Synthesis of *mer*-$Re(OPPh_3)Cl_3$(RB), 3. The complexes could be prepared in 75−80% yield by the two methods outlined below, which differ in the oxidant used. Details are given for one representative case.

Trichloro(triphenylphosphine oxide)(*N*-*p*-tolyl-2-picolinamide)rhenium(IV), *mer*-$Re(OPPh_3)Cl_3$(MeB), 3(Me). a. Hydrogen Peroxide Method. $Re(OPPh_3)Cl_3$(MeA) (50 mg, 0.07 mmol) was dissolved in 20 mL of acetonitrile, and 0.25 mL of H_2O_2 (30%) was added. The solution was stirred for 1 h, during which the color became brownish-yellow. Evaporation of the solution under reduced pressure gave a brown solid, which was repeatedly washed with water and dried in vacuo over P_4O_{10}. The product, $Re(OPPh_3)Cl_3$(MeB), thus obtained was recrystallized from toluene. Yield: 35 mg, 75%. Anal. Calcd for $Re(OPPh_3)Cl_3$(MeB), $ReC_{31}H_{26}N_2Cl_3O_2P$: C, 47.60; H, 3.33; N, 3.58. Found: C, 47.67; H, 3.28; N, 3.64.

b. Cerium(IV) Method. To a solution of 100 mg (0.13 mmol) of $Re(OPPh_3)Cl_3$(MeA) in 30 mL dichloromethane−acetonitrile (1:6) was added 200 mg (0.31 mmol) of $[NH_4]_4[Ce(SO_4)_4]\cdot 2H_2O$ dissolved in 20 mL of water. The mixture was stirred at room temperature for 2 h. The supernatant brownish-yellow solution was decanted, separating it from the yellow colloidal suspension containing cerium(III). The solution was evaporated to dryness under reduced pressure. The brown solid product thus obtained was repeatedly washed with water and then dried in vacuo over P_4O_{10}. Yield: 81 mg, 80%. Anal. Calcd for $Re(OPPh_3)Cl_3$(MeB), $ReC_{31}H_{26}N_2Cl_3O_2P$: C, 47.60; H, 3.33; N, 3.58. Found: C, 47.56; H, 3.38; N, 3.51.

Anal. Calcd for $Re(OPPh_3)Cl_3$(HB), $ReC_{30}H_{24}N_2Cl_3O_2P$: C, 46.90; H, 3.13; N, 3.65. Found: C, 46.94; H, 3.17; N, 3.60. Calcd for $Re(OPPh_3)Cl_3$(ClB), $ReC_{30}H_{23}N_2Cl_4O_2P$: C, 44.89; H, 2.87; N, 3.49. Found: C, 44.84; H, 2.92; N, 3.54. Calcd for $Re(OPPh_3)Cl_3$(OMeB), $ReC_{31}H_{26}N_2Cl_3O_3P$: C, 46.64; H, 3.26; N, 3.51. Found: C, 46.60; H, 3.20; N, 3.46.

Kinetic Measurements. a. The Reaction 1 → 2. A known excess of PPh_3 was added to a solution of **1**(Me) (2.4×10^{-4}−2.7×10^{-4} M) in dichloromethane at the desired temperature, and the reaction was followed spectrophotometrically by measuring the increase in absorbance of the peak at 680 nm of the complex $Re(OPPh_3)Cl_3$(MeA) with time. This was done using different PPh_3 concentrations for a fixed concentration of **1**(Me). The absorption, A_t, was digitally recorded as a function of time, t, and A_α was measured (after 24 h) when the

(24) (a) Margerum, D. W. *Pure Appl. Chem.* **1983**, *55*, 23. (b) Workman, J. M.; Powel, R. D.; Procyk, A. D.; Collins, T. J.; Bocian, D. F. *Inorg. Chem.* **1992**, *31*, 1548. (c) Chandra, S. K.; Chakravorty, A. *Inorg. Chem.* **1992**, *31*, 760.
(25) Chatt, J.; Rowe, G. A. *J. Chem. Soc.* **1962**, 4019.
(26) Bähr, G.; Thamlitz, H. *Z. Anorg. Allg. Chem.* **1955**, *282*, 3.
(27) (a) Basu, P.; Bhanja Choudhury, S.; Chakravorty, A. *Inorg. Chem.* **1989**, *28*, 2680. (b) Ray, D.; Chakravorty, A. *Inorg. Chem.* **1988**, *27*, 3292.
(28) Pramanik, A.; Bag, N.; Lahiri, G. K.; Chakravorty, A. *Inorg. Chem.* **1991**, *30*, 410.

Table 6. Crystallographic Data for *mer*-$ReOCl_3$(MeA), **1**(Me)

empirical formula	$C_{13}H_{12}Cl_3N_2ORe$	V, Å^3	782.5(8)
fw	504.8	Z	2
space group	$P\bar{1}$	T, °C	22
a, Å	7.136(4)	λ, Å	0.710 73
b, Å	8.329(5)	ρ_{obsd}, g cm^{-3}	2.139
c, Å	14.104(9)	ρ_{calcd}, g cm^{-3}	2.143
α, deg	73.88(5)	μ, cm^{-1}	82.7
β, deg	76.35(5)	R,[a] %	4.86
γ, deg	85.64(5)	R_w,[b] %	5.76

[a] $R = \sum||F_o| - |F_c||/\sum|F_o|$. [b] $R_w = [\sum w(|F_o| - |F_c|)^2/\sum w|F_o|^2]^{1/2}$; $w^{-1} = \sigma^2(|F_o|) + g|F_o|^2$; $g = 0.0005$.

reaction was complete. Values of the pseudo-first-order rate constants (k_{5obs}) were obtained from the slopes of the highly linear plots of $-\ln(A_\alpha - A_t)$ versus t. A minimum of 30 $A_t - t$ data points were used in each calculation. Values of the second-order rate constants (k_5) were obtained from the slopes of the excellently linear plots of k_{5obs} versus [PPh_3]. The activation enthalpy and entropy parameters were calculated from the Eyring equation (13) utilizing rate constant data obtained over the temperature range 287−299 K.

$$k_5 = (k_B T/h)[\exp(-\Delta H^{\ddagger}/RT)\exp(\Delta S^{\ddagger}/R)] \quad (13)$$

b. The Reaction $2^+ \rightarrow 3$. The compound $Re(OPPh_3)Cl_3$(MeA), **2**(Me), was quantitatively oxidized to $\mathbf{2}^+$(Me) via coulometry at +0.5 V versus SCE in scrupulously dry acetonitrile. Aliquots of this solution were diluted as required, and measured amounts of water were added using a calibrated microsyringe. The reaction was followed spectrophotometrically at 680 nm, and the corresponding pseudo-first-order rate constant (k_{6obs}) values were obtained from the absorbance versus time trace by the procedure described above. Keeping the concentration of **2**(Me) fixed and varying the water concentration, we repeated the experiment three times at each temperature. The second-order rate constant (k_6) was determined from the slope of the straight line obtained by plotting k_{6obs} versus [H_2O]. The activation parameters, $\Delta H^{\ddagger}$ and $\Delta S^{\ddagger}$ were obtained from variable-temperature (280−299 K) rates using the Eyring equation (13).

X-ray Structure Determination. Dark prismatic crystals of dimensions 0.50 × 0.40 × 0.20 mm^3 for $ReOCl_3$(MeA) were grown by slow diffusion of hexane into a dichloromethane solution of the complex at 298 K.

Cell parameters were determined by a least-squares fit of 30 machine-centered reflections ($2\theta = 15-30°$). Data were collected by the ω-scan technique in the range $3° \le 2\theta \le 50°$ on a Siemens R3m/V four-circle diffractometer with graphite-monochromated Mo Kα radiation. Two check reflections monitored every 198 reflections showed no significant change in intensity after the required 22 h of exposure to X-rays. All data were corrected for Lorentz−polarization and absorption.[29] Of the 2798 ($h = 0, 8$; $k = \pm 9$; $l = -15, 16$) reflections collected, 2759 were unique, of which 2336 were taken as observed ($I > 3\sigma(I)$) for structure solution and refinement. The cell was triclinic, and the structure was successfully solved in the $P\bar{1}$ space group.

The metal atoms were located from Patterson maps, and the rest of the non-hydrogen atoms emerged from successive Fourier syntheses. The structures were then refined by full-matrix least-squares procedures. All non-hydrogen atoms were refined anisotropically. Hydrogen atoms were included in calculated positions with fixed thermal parameters ($U = 0.08$ Å^2). All calculations were done on a Micro VAX II computer using the SHELXTL-PLUS Program Package.[30] Significant crystal data are listed in Table 6.

Acknowledgment. We thank the Department of Science and Technology, Indian National Science Academy, and the Council of Scientific and Industrial Research, New Delhi, for financial support. Affiliation with the Jawaharlal Nehru Centre for Advanced Scientific Research, Bangalore, India, is acknowledged.

Supporting Information Available: For $ReOCl_3$(MeA), crystallographic data (Table S1), atomic coordinates and equivalent isotropic coefficients (Table S2), complete bond distances (Table S3) and angles (Table S4), anisotropic thermal parameters (Table S5), hydrogen atom positional parameters (Table S6), and time-dependent spectra and Erying plots (Figure S1) (8 pages). Ordering information is given on any current masthead page.

IC9611094

(29) North, A. C. T.; Philips, D. C.; Mathews, F. S. *Acta Crystallogr.* **1968**, *A24*, 351.
(30) Sheldrick, G. M. *SHELXTL-PLUS 88, Structure Determination Software Programs*; Siemens Analytical X-ray Instruments Inc.: Madison, WI, 1990.